Quaternary Science Reviews 192 (2018) 236–248

Contents lists available at ScienceDirect

Quaternary Science Reviews

journal homepage: www.elsevier.com/locate/quascirev

# Vegetation responses to the warming at the Younger Dryas-Holocene transition in the Hengduan Mountains, southwestern China

Xia Wang [a, d], Yi-Feng Yao [a, *], Alexandra H. Wortley [b], Hui-Jie Qiao [c], Stephen Blackmore [b], Yu-Fei Wang [a, **], Cheng-Sen Li [a]

[a] State Key Laboratory of Systematic and Evolutionary Botany, Institute of Botany, Chinese Academy of Sciences, Beijing, 100093, China
[b] Royal Botanic Garden Edinburgh, 20a Inverleith Row, Edinburgh, EH35LR, Scotland, UK
[c] Institute of Zoology, Chinese Academy of Sciences, Beijing, 100101, China
[d] University of Chinese Academy of Sciences, Beijing, 100049, China

ARTICLE INFO

*Article history:*
Received 25 April 2018
Received in revised form
4 June 2018
Accepted 4 June 2018
Available online 11 June 2018

*Keywords:*
Biodiversity conservation
Biotic feedback
China
Climate change
Global warming
Holocene
Micropaleontology
Pollen
Paleoclimatology
Vegetation dynamics

ABSTRACT

The Younger Dryas (YD) is one of the most abrupt climatic events in Earth's recent history. The warming at the end of the YD, in particular, is considered to be comparable to the global warming seen in the 21st century. However, the YD termination has received little attention, particularly in the Hengduan Mountains of Southwestern China, a low latitude temperate biodiversity hotspot. Here we present evidence for a rapid response in the diversity and composition of vegetation to the warming at the YD termination, based on a continuous, well-dated pollen sequence and loss-on-ignition data (12.9–9.2 cal. ka BP) from Haligu wetland in the Hengduan Mountains. Our data indicate that variations in plant diversity were correlated with relative humidity during this period, and suggest a distinct shift from *Pinus-Abies-Picea* forest to *Pinus*-dominated forest at the YD-Holocene transition, accompanied by an increase in coverage of generally temperate taxa such as *Salix* and *Betula*. This finding provides insights that may be of relevance to biodiversity conservation under future warming scenarios in similar mountain ecosystems worldwide.



## 1. Introduction

The Younger Dryas (YD, ca. 12.8–11.5 cal. ka BP (before present, 0 BP = 1950 AD)) is the most recent abrupt climatic event recognized during the transition from the last glaciation to the Holocene (Jomelli et al., 2014; Partin et al., 2015) and has been very widely observed in marine and continental sediments in the North Atlantic, North Pacific, Asia, North America, tropical regions, and the Southern Hemisphere (e.g., Johnsen et al., 1992; Dansgaard et al., 1993; Bond et al., 1993; Clark et al., 2002; Shakun and Carlson, 2010). At middle and high latitudes in North America and Europe, changes in the biota, including humans and other terrestrial mammals, have been observed in response to the YD event. For example, in regions of Southwestern North America the YD climate change was accompanied by significant changes from Clovis to Folsom cultures marked by a shift from hunting mammoth to bison (Ballenger et al., 2011). In North America, large mammals such as *Mammuthus*, *Arctodus* and *Smilodon* became extinct during this period (Barnosky et al., 2004). In Romania, diatom responses to the YD have been recorded from lake sediments, including changes in the relative abundance of *Staurosira venter* (Ehr.) Cleve & Moeller and *Stauroforma exiguiformis* (Lange-Bertalot) Flower, along with an overall decrease in diversity (Buczkó et al., 2012). However, few studies are available at low latitudes (e.g., Rull et al., 2010; Ivory et al., 2012). Specifically, the abrupt warming at the YD termination received significantly little attention.

The temperate Hengduan Mountains of Southwestern China are located at the southeastern margin of the Qinghai-Tibet Plateau (Fig. 1a) and form one of 34 designated global biodiversity hotspots (Boufford and van Dijk, 2004). Climatic oscillations within Quaternary glacial and interglacial periods are inferred to have had significant effects on plant diversity and distributions in the north

* Corresponding author.
** Corresponding author.
*E-mail addresses:* yaoyf@ibcas.ac.cn (Y.-F. Yao), wangyf@ibcas.ac.cn (Y.-F. Wang).

https://doi.org/10.1016/j.quascirev.2018.06.007
0277-3791/

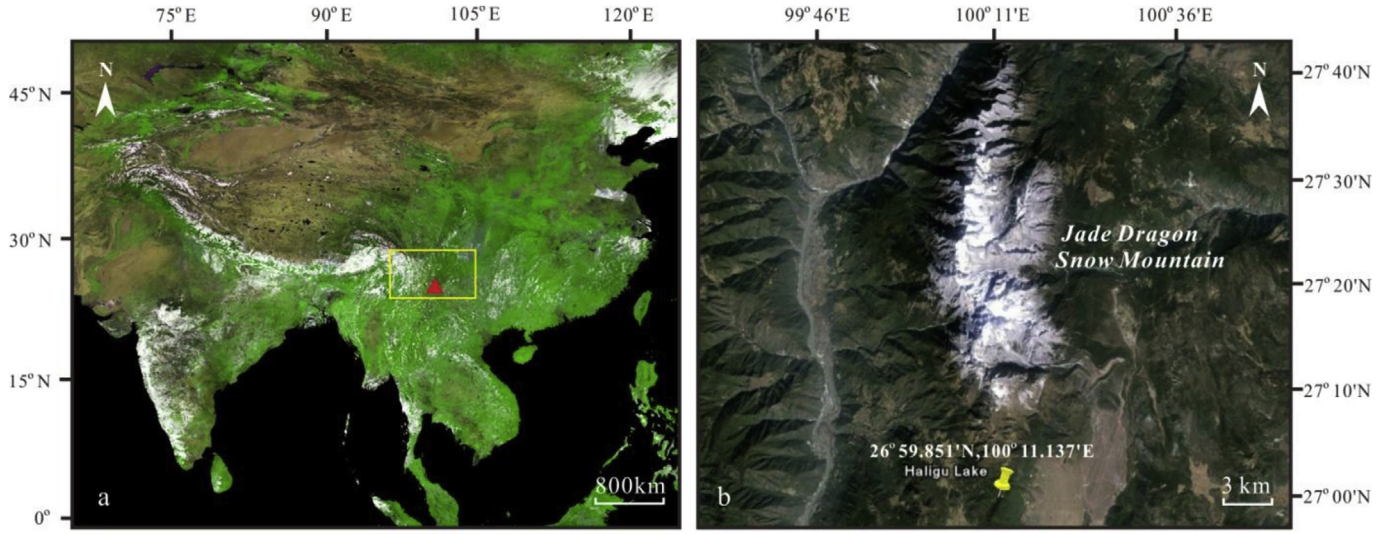


**Fig. 1.** Location of the study site. a. Location of the Hengduan Mountains (yellow rectangle) and position of coring site (red triangle). Map obtained by European Space Agency satellite Proba-V (June 2013). b. Location of coring site at Haligu on the Jade Dragon Snow Mountain. Image from Google Earth. (For interpretation of the references to colour in this figure legend, the reader is referred to the Web version of this article.)

and south of this region (Wu, 1988; Sun, 2002). In the Hengduan area itself, previous studies have mostly concentrated on vegetation succession, climate change and the evolution of the monsoon during the late Quaternary (e.g., Shen et al., 2006; Kramer et al., 2010; Xiao et al., 2014a, 2014b; Rawat et al., 2015; Zhang et al., 2015; Yao et al., 2015, 2017), but little is known about how plant communities responded to the YD event, particularly the rapid warming at the YD termination, which is regarded as providing a potential analog for predicted future global warming (Rull et al., 2015). Here, we present a high-resolution pollen and loss-on-ignition (LOI) record from a wetland site at Haligu (3218 m a. s. l.), and use it to investigate the impacts of abrupt climate shifts at the YD-Holocene transition on plant community composition in the Hengduan Mountains. The study aims to 1) improve understanding of the YD climatic reversal and late glacial-Holocene transition in the Hengduan Mountains, and 2) provide a past analog for biotic responses to potential climatic developments similar to the rapid climatic shifts seen in the YD-Holocene under near-future global warming caused by anthropogenic activity. This may facilitate the formulation and adoption of present and future biodiversity conservation policies.

## 2. Materials and methods

### 2.1. Study site

The floristically diverse Jade Dragon Snow Mountain is located in the Hengduan Mountains, within the subtropical South Asian monsoon zone, which is influenced by heat and water sources from the South China Sea and the Indian Ocean. Thus the summers are warm and humid and the winters cool and dry. At the nearest official weather station in Lijiang (about 17 km far from the Jade Dragon Snow Mountain, 2200 m a. s. l.), the mean annual precipitation is 935 mm and more than 90% of the annual precipitation falls in summer, from June to October. The mean annual temperature is 12.8 °C, and the warmest month is July, with a mean temperature of 17.9 °C; the coldest month is January, with a mean temperature of 5.9 °C (Feng et al., 2006). The local vegetation displays a distinct vertical zonation. Between 2400 m a. s. l. and 3000 m a. s. l., the vegetation is dominated by semi-humid evergreen broad-leaved forest-pine forest. From 3000 m a. s. l. to 3300 m a. s. l., the vegetation succeeds to needle- and broad-leaved mixed forest-sclerophyllous evergreen broad-leaved forest. From 3300 to 4200 m a. s. l., it comprises cold-temperate coniferous forest, and above 4200 m the vegetation changes to alpine shrub meadow (Yao et al., 2015). The present-day vegetation of the study area is dominated by needle-leaved trees (such as *Pinus yunnanensis* Franch.) and evergreen oak (*Quercus aquifolioides* Rehd. et Wils.) along with deciduous broad-leaved trees such as *Populus davidiana* Dode., *Acer davidii* Franch., and *Rhododendron* spp., especially *R. mucronatum* (Blume) G. Don, *R. racemosum* Franch., *R. yunnanense* Franch. and *R. delaveyi* Franch. At higher elevations important tree species comprise *Abies delavayi* Franch., *Picea likiangensis* (Franch.) Pritz., and *Tsuga dumosa* (D. Don) Eichler (Wang et al., 2007).

### 2.2. Sampling and dating

In October 2008, a sediment core 730 cm in length was obtained using a Russian corer at Haligu (26°59.851′ N, 100°11.137′ E, 3218 m a. s. l., Fig. 1b) on the southern end of the Jade Dragon Snow Mountain. The core was documented and wrapped in PVC tubes in the field. The present study focuses on the lower part of the core (730–510 cm), which comprises black and grey-brown clays. In total, nine AMS (Accelerator Mass Spectrometry) radiocarbon dates were obtained from the core by the Scottish Universities Environmental Research Centre (SUERC) in Glasgow, Scotland and Beta Analytic Radiocarbon Dating Laboratory in Florida, USA, at depths of 100 cm, 200 cm, 300 cm, 400 cm, 500 cm, 550 cm, 600 cm, 700 cm, and 730 cm. Because there are no fragments of plant material suitable for analysis in the core, bulk samples were used. The $^{14}C$ age is quoted in conventional years BP; age calibration was achieved using OxCal v3.10 (Baillie and Reimer, 2004; Bronk, 2005). Errors are expressed at the two sigma level of confidence (95% probability), the end points of the dates were rounded to the nearest 10 years, and dates are quoted in calibrated years BP (Mook, 1986; Foster et al., 2008). Radiocarbon dating results are shown in Table 1.

**Table 1**
AMS$^{14}$C dating results for the Haligu core.

| Lab code | Depth (cm) | $\delta^{13}C$ | $^{14}C$ date (yr BP) | Calibrated age (cal. yr BP, 2σ) | Mid-point (cal. yr BP) |
|---|---|---|---|---|---|
| SUERC-23561 | 100 | −27.3‰ | 965 ± 30 | 940–790 | 865 |
| SUERC-23562 | 200 | −26.6‰ | 2215 ± 30 | 2330–2150 | 2240 |
| SUERC-23563 | 300 | −27.9‰ | 2625 ± 30 | 2785–2720 | 2750 |
| SUERC-23564 | 400 | −27.6‰ | 5150 ± 30 | 5990–5750 | 5870 |
| SUERC-23568 | 500 | −27.3‰ | 7980 ± 35 | 9000–8700 | 8850 |
| Beta-469912 | 550 | −26.7‰ | 9020 ± 30 | 10236–10177 | 10207 |
| SUERC-23569 | 600 | −26.4‰ | 9745 ± 35 | 11240–11120 | 11180 |
| SUERC-23570 | 700 | −26.9‰ | 10520 ± 35 | 12690–12380 | 12535 |
| Beta-469914 | 730 | −27.1‰ | 10430 ± 40 | 12437–12107 | 12272 |
| | | | | 12526–12460 | 12493 |

### 2.3. Laboratory methods

In total, one hundred and ten samples were extracted, at 2 cm intervals, for palynological investigation and LOI analysis.

For pollen analysis, five grams of each sample were treated by heavy liquid separation (Moore et al., 1991). One tablet of *Lycopodium* spores (batch: 2013001; 27,560 ± 2643 spores/tablet) was added to each sample before treatment, to enable us to calculate the pollen concentration. Pollen influx data are an estimation of the amount of pollen grains deposited annually in single unit surface (Berglund and Ralska-Jasiewiczowa, 1986), which are estimated based on the pollen concentration and sedimentation rates inferred from the constructed age-depth model. At least 400 spores and pollen grains were counted for each sample, together with the *Lycopodium* spores, under a Leica DM 2500 light microscope at a magnification of 400 ×. Identification of palynomorphs was performed by comparison with palynological monographs (IBCAS, 1976; IBSC-IBCAS, 1982; Wang et al., 1995). SEM imaging of single pollen grains was conducted with a Hitachi S-4800 Field Emission Scanning Electron Microscope at the Institute of Botany, Chinese Academy of Sciences, Beijing. Spores and pollen grains were allocated to four categories: coniferous trees, broad-leaved trees and shrubs, herbs, and ferns. Calculation of relative abundance, pollen concentration and influx, and pollen diagram plotting, were carried out using TILIA 1.7.16 and TILIA.GRAPH (Grimm, 2011). Division of the core into pollen zones was based on the results of a Constrained Incremental Sums of Squares (CONISS) cluster analysis conducted in TILIA.

For LOI analysis, five grams of each sample were dried in a porcelain crucible for 12 h at 105 °C and combusted for 2 h at 550 °C within a muffle furnace (Dean, 1974). The organic matter content was calculated as follows: $LOI_{550} = (M_{105} - M_{550})/(M_{105} - M_0) \times 100\%$ ($M_0$: the net weight of crucible, $M_{105}$: weight of dried sample and crucible, $M_{550}$: weight of sample and crucible after combustion at 550 °C).

### 2.4. Numerical analysis

Twenty-four species of terrestrial plant pollen types (aquatic plants and ferns excluded) with relative abundances of at least 1% in at least one sample, were selected for numerical analysis using CANOCO 4.5 (ter Braak and Smilauer, 2002). We used detrended correspondence analysis (DCA) to determine whether a linear model or a unimodal model was needed. In the DCA analysis, a maximum gradient value of less than three in four axes suggests that the response of pollen assemblages to environment variables follows a linear relationship; a value of more than four suggests that a unimodal model is appropriate; and a value between three and four indicates that both linear and unimodal models are suitable. The maximum gradient obtained was 1.255; thus, we used linear principal component analysis (PCA) to investigate the relationship between pollen assemblages and environmental factors (Birks and Gordon, 1985). For PCA, species data were subjected to square root transformation and centering/standardization following Birks and Gordon (1985) and Frey and Deevey (1998).

### 2.5. Determination of plant taxonomic diversity

In order to investigate changes in plant diversity and its response to climate change during the YD in the study area, we used pollen data (for all palynomorphs recovered from each sample, including ferns and aquatics) to represent the plant diversity of each sample. Please note that usually fossil pollen was identified to genus or family level and each pollen type may represent more than one plant taxon, so the actual plant species diversity in the sediment deposition period may be higher than that estimated by pollen data. Plant diversity at different depths was quantified using the Vegan 2.4 package in R (Oksanen et al., 2016). Diversity was calculated using the Simpson index, Shannon–Wiener index, Pielou's evenness index, and species richness, using formulae as follows:

(1) Simpson index = 1−sum pi^2 (gives values between 0 and 1 with higher values indicating higher diversity);
(2) Shannon–Wiener index = −sum pi log (b) pi (pi: the relative abundance of pollen type I, b: radix of logarithm);
(3) Species richness = number of species in each sample. To avoid artefacts due to differing total pollen counts (Miller and Foote, 1996), calculations were limited to 421 grains or spores (the number found in the smallest sample) per sample, based on Sanders (1968);
(4) Pielou's evenness (the relative abundance of each species in each sample) = Shannon–Wiener index/log (species richness).

Rarefaction analysis (Sanders, 1968) was used to compare species richness for the samples collected between the present, early Holocene (9.3–9.1 ka BP), YD (12.5 ka BP), and before the YD (Older Dryas) in the study area. Data for surface soil samples were taken from Song et al. (2012), data for the early Holocene (9.3–9.1 ka BP) and YD (12.5 ka BP) from this study, and data for before the YD were obtained from a core at Wenhai Lake, about 2 km from Haligu (Yao et al., 2015). Boxplots were used to compare species richness across samples representing different time periods.

## 3. Results

### 3.1. Chronology and sedimentation

An age-depth model (Fig. 2) for the studied Haligu core was constructed using the Bayesian age-depth modelling software Bacon (version 2.2, Blaauw and Christen, 2011) in R (version 3.1.2, R

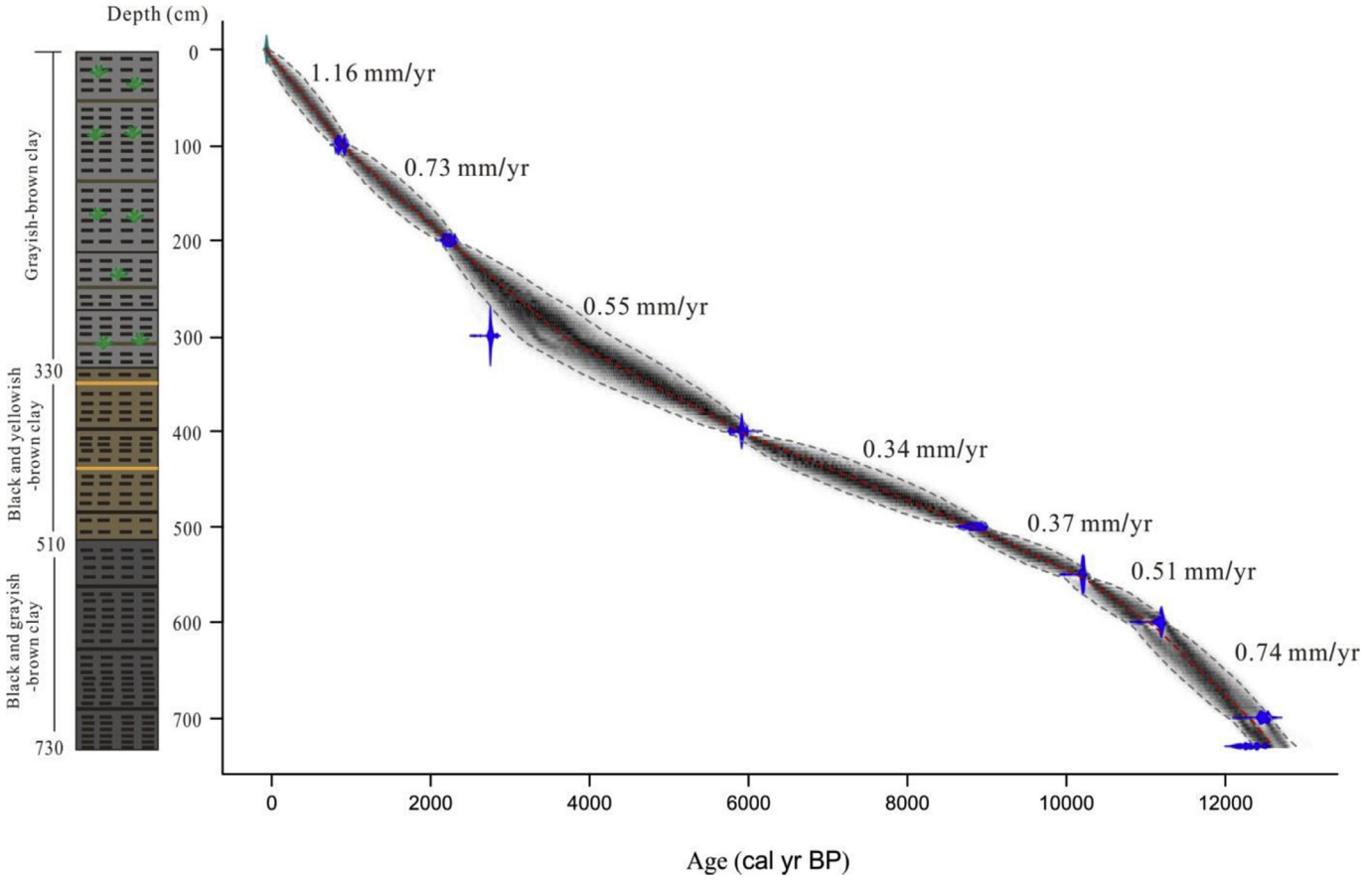


**Fig. 2.** Age-depth model for the Haligu core.

Core Team, 2014) based on nine AMS $^{14}$C dates (Table 1). The model shows sediment-accumulation rates of 0.74 mm/yr for the depth range 730–600 cm, 0.51 mm/yr for 600–550 cm and 0.37 mm/yr for 550–510 cm. Ages at other depths were estimated by interpolation and extrapolation. The 730–510 cm section of the core was estimated to correspond to 12.9–9.2 cal. ka BP, i.e., it encompasses the YD and early Holocene. According to the sedimentation rates, each sample represents ca. 27 years for 730–600 cm, 39 years for 600–550 cm, and 54 years for 550–510 cm.

### 3.2. Pollen assemblages and vegetation composition

All samples were abundant in palynomorphs, showing a high degree of taxonomic diversity (Figs. S1-S5). In total, 60,590 spores and pollen grains were identified and were assigned to 77 taxa (52 families and 25 genera; Table S1). However, the actual number of plant taxa contributing to the pollen rain during the course of the sediment deposition period may well have been higher, because many of the fossil pollen types recognized represent more than one species or genus. Based on the relative abundance and pollen concentration of the dominant taxa, and a cluster analysis of all taxa using CONISS, the 730–510 cm section of the core was divided into five distinct palynological zones (PZ, Figs. 3 and 4). The features of each zone are described as follows:

**PZ 1** (730–690 cm; 12.9–12.4 cal. ka BP): The mean relative abundances of *Picea* (5.0%) and *Abies* (30.2%) are the highest encountered in the five zones and are accompanied by a low abundance of *Tsuga* (0.4%) pollen. Flowering plants mainly comprise Cyperaceae (6.1%) and Fabaceae (2.6%). Ferns are dominated by Polypodiaceae (6.6%) and Athyriaceae (1.4%). Total pollen concentration is the lowest of all the zones (mean 6921 grains/g). Total index values vary between 110 and 1385. The palynological assemblage is inferred to correspond to a vegetation dominated by needle-leaved forest (mainly *Pinus, Abies,* and *Picea*), together with a small number of broad-leaved taxa such as *Quercus*, *Betula,* and *Corylus.* Plant diversity undergoes a distinct decrease to 12.7 cal. ka BP followed by an increase (Fig. 5e–h). Rarefied richness fluctuates between 16 and 28 species per sample (mean 22), reaching its lowest value at ca. 12.7 cal. ka BP.

**PZ 2** (690–650 cm; 12.4–11.9 cal. ka BP): In this zone, the main characteristic is a decrease in *Picea* (falling to 1.1%) and *Abies* pollen (falling to 23.1%) and significant increase in *Tsuga* pollen (up to 3.4%). Flowering plants such as *Castanopsis*, *Tilia,* and Oleaceae occur for the first time, all at percentages below 1%. Total pollen concentration sharply increases to 12,839 grains/g. Total index values vary between 416 and 1948. In terms of the vegetation assemblage, the composition of the needle-leaved forest is inferred to have changed to *Pinus*, *Abies,* and *Tsuga*. Plant diversity again experiences a notable decrease to 12.1 cal. ka BP followed by an increase, with a higher mean value of each index (e.g. rarefied richness is 26 species/sample), implying a higher overall plant species diversity than in PZ 1 (Fig. 5e–h).

**PZ 3** (650–604 cm; 11.9–11.2 cal. ka BP): This zone is characterized by a decrease in *Tsuga* (falling to 0.9%) and Cyperaceae pollen (falling to 1.3%), and an increase in Asteraceae pollen (up to 2.1%). The relative abundances of *Picea* (2.1%) and *Abies* pollen (21.9%) are similar to the proceeding stage. *Castanea* pollen reaches its highest value (11.6%) for all zones. Total pollen concentration

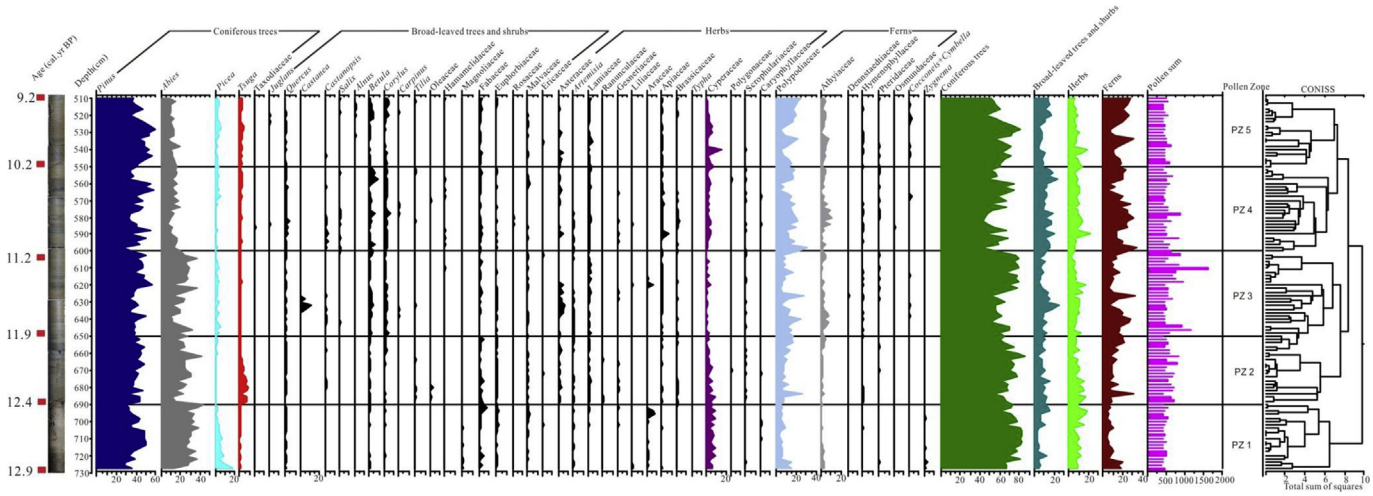


**Fig. 3.** Diagram showing changes in relative abundance (expressed in %) for the major palynomorphs recovered from the Haligu core.

continues to increase (mean 16,195 grains/g). Total index values vary between 525 and 2450. The vegetation is still dominated by needle-leaved forest (mainly *Pinus* and *Abies*). Once again plant diversity first increases to 11.4 cal. ka BP and then decreases (Fig. 5e–h). Although each index fluctuates significantly, the mean values (e.g. rarefied richness is 27 species/sample) indicate a similar diversity to PZ 2.

**PZ 4** (604–550 cm; 11.2–10.2 cal. ka BP): The major feature of this zone is a notable decrease in *Abies* pollen (falling to 13.7%), along with an increases in Cyperaceae pollen (up to 2.8%), and Polypodiaceae (up to 14.7%) and Athyriaceae spores (up to 3.5%). The total pollen concentration is lower than in PZ 3 (mean 13,564 grains/g). Total index values vary between 189 and 1462. As in the previous stage, the vegetation is dominated by *Pinus* and *Abies*, but the overall plant diversity is the highest of all the zones (Fig. 5e–h), with a peak rarefied richness value (35 species/sample, mean 28) occurring at ca. 10.2 cal. ka BP.

**PZ 5** (550–510 cm; 10.2–9.2 cal. ka BP): In this zone, the most distinctive characteristic is the continued decrease in *Abies* pollen (falling to 11.6%), accompanied by relatively high values for Polypodiaceae (mean 13.8%) and Athyriaceae spores (mean 3.8%). Cyperaceae pollen reaches its highest value (16.0%) at ca. 9.8 cal. ka BP. Total pollen concentration decreases to 12,098 grains/g. Total index values vary between 75 and 696. Index curves show that the plant diversity experiences a decrease at the beginning of this zone, followed by an increase from 9.7 cal. ka BP (Fig. 5e–h). The floristic diversity is lower than in PZ 4, suggested by the relatively low mean value of each index (e.g. rarefied richness 25 species/sample).

### 3.3. Comparison of plant diversity

We used a rarefaction analysis to estimate species richness based on pollen data from selected samples in order to compare plant diversity in the periods pre-YD (Older Dryas, OD; 17.1–16.3 cal. ka BP), YD (ca. 12.5 cal. ka BP), post-YD (Early Holocene, EH; 9.4–9.2 cal. ka BP) and the present (P). Rarefied curves indicate that species richness fluctuates between 19 and 28 species per sample for the 421 counted pollen grains during the YD. Rarefied richness is highest in the EH (25–28 species), and there is no statistically significant difference between samples from the YD and OD (YD: 19–28 species, OD: 20–26 species). The rarefied richness of surface (present day) samples is significantly different (lower) to the other samples (10–16 species, Tukey test, $P < 0.001$; Figs. 6 and 7).

### 3.4. LOI analysis

The relative variations of LOI in the present study represent the characteristics of the organic matter content during the deposition period (12.9–9.2 cal. ka BP). In PZ1, the LOI value undergoes a distinct decrease around 12.9 cal. ka BP followed by an increase (Fig. 5c), ranging from 15.0% to 58.6% (mean 36.4%). In PZ2, the LOI value again shows a notable decrease to 12.2 cal. ka BP followed by an increase, with a lower mean value (26.3%) compared to PZ1, and notably reaching its lowest value (13.8%) at 12.2 cal. ka BP (Fig. 5c). In PZ3, the LOI value first increases to 11.5 cal. ka BP and then decreases (Fig. 5c), fluctuating between 20.4% and 55.0% (mean 30.1%). In PZ4, the LOI value changes from 15.8% to 50.2% (27.6%) (Fig. 5c). In PZ5, the mean value of LOI is the highest (41.2%) of all zones, attaining a peak value (61.0%) around 9.9 cal. ka BP (Fig. 5c).

### 3.5. Numerical analysis and climate oscillation

The results of a PCA of 24 terrestrial pollen types reveal that the first two axes capture 83% of the variance in the pollen data, viz., axis 1 captures 52.5% of the variance and axis 2 captures 30.5% (Fig. 8a). The cold-tolerant needle-leaved taxa *Picea* and *Abies* are located at the positive end of axis 1, while *Pinus* and the temperate broad-leaved taxa *Betula, Corylus, Salix, Alnus,* and *Castanea* are located at the negative end of axis 1 (Fig. 8a), so this axis is inferred to represent the ordination of temperature from warm (negative) to cold (positive). The hygrophilous broad-leaved taxon *Alnus* and most temperate broad-leaved taxa such as *Quercus, Castanea,* and *Salix* lie towards the positive end of axis 2, while drought-tolerant needle-leaved taxa such as *Pinus* and *Abies* lie towards the negative end of axis 2 (Fig. 8a). We therefore infer that axis 2 represents the ordination of relative humidity from dry (negative) to wet (positive).

In the PCA plot, almost all samples in PZ 1 (samples 91–109, the exception being 110) and most samples in PZ 2 (samples 71–90) and PZ 3 (samples 48–70) are located towards the positive end of axis 1. Samples in PZ 4 (samples 21–47, except for 46 and 47) and PZ 5 (samples 1–20) lie towards the negative end of axis 1 (Fig. 8b). Examining the scores for all samples along axes 1 (PCA1) and 2 (PCA2) shows the changes in temperature and relative humidity inferred during the transition from the YD to the early Holocene (Fig. 5a and d). This suggests cold conditions in PZ 1, temperature fluctuations in PZ 2 and PZ 3, and warm environments in PZ 4 and

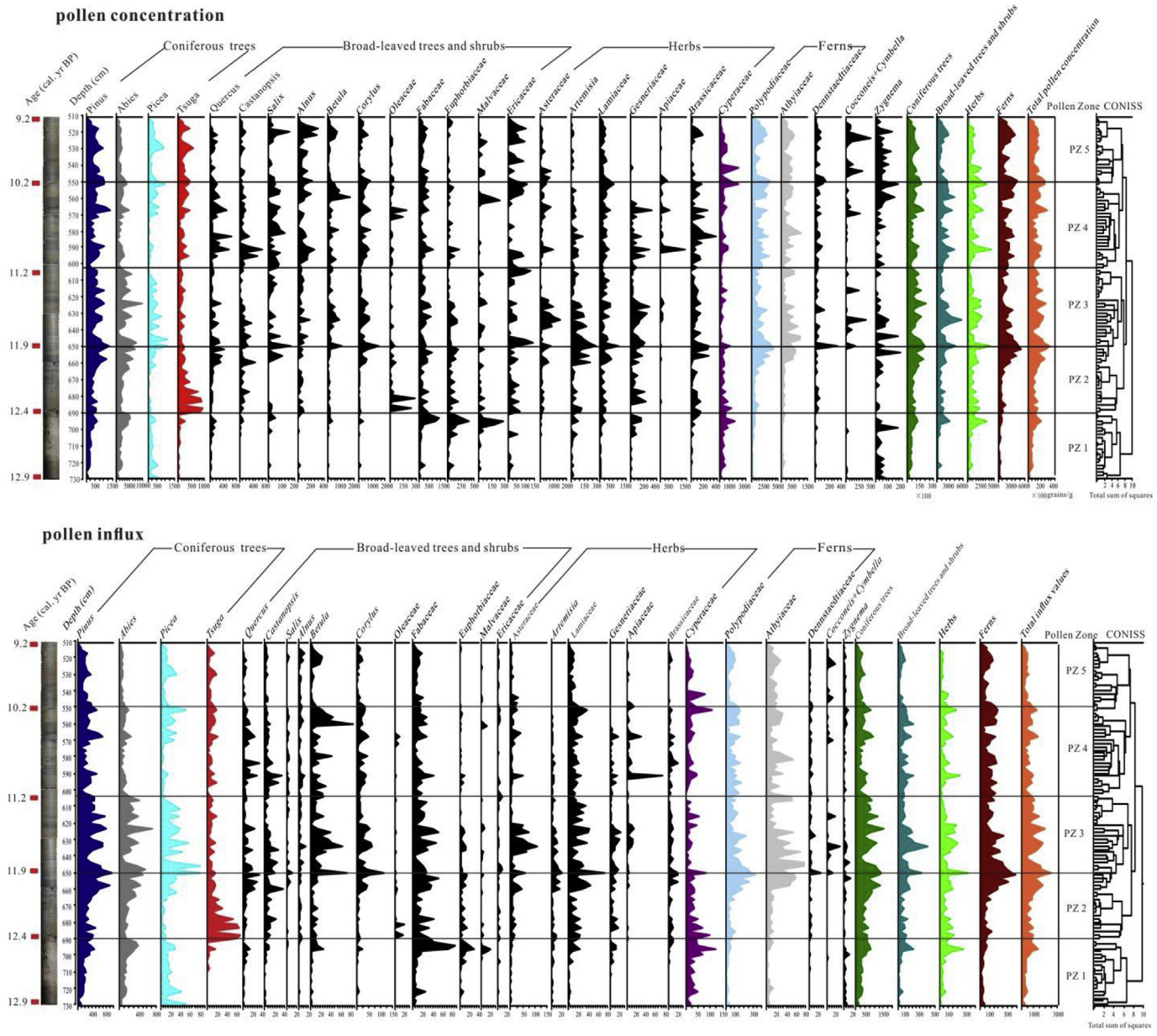


**Fig. 4.** Diagram showing variations in pollen concentration (top) and influx (bottom) for the major palynomorphs recovered from the Haligu core.

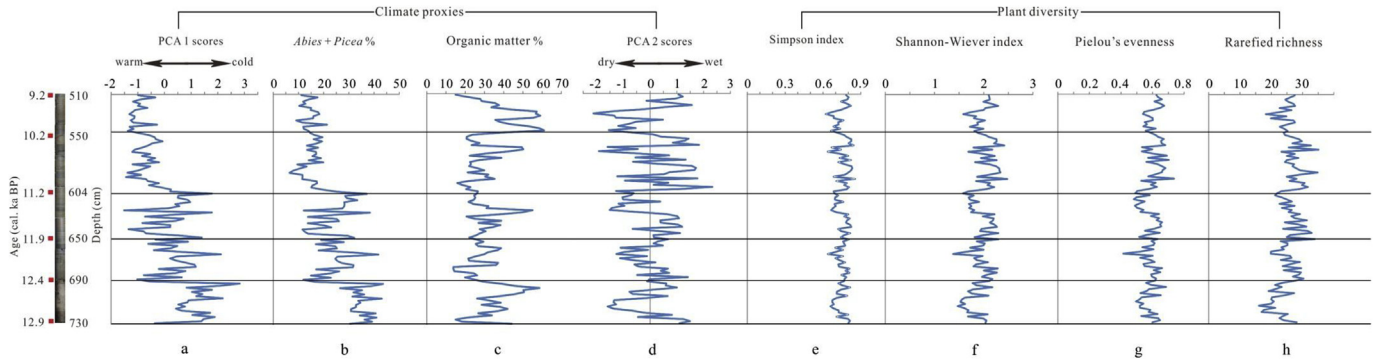


**Fig. 5.** Curves showing plant diversity in relation to climatic changes from the Younger Dryas (YD) to the early Holocene (12.9–9.2 cal. ka BP). a. PCA 1 scores. b. Relative abundance of *Abies* and *Picea* pollen. c. LOI values, d. PCA 2 scores. e. Simpson index. f. Shannon-Wiener index. g. Pielou's evenness. h. Rarefied richness.

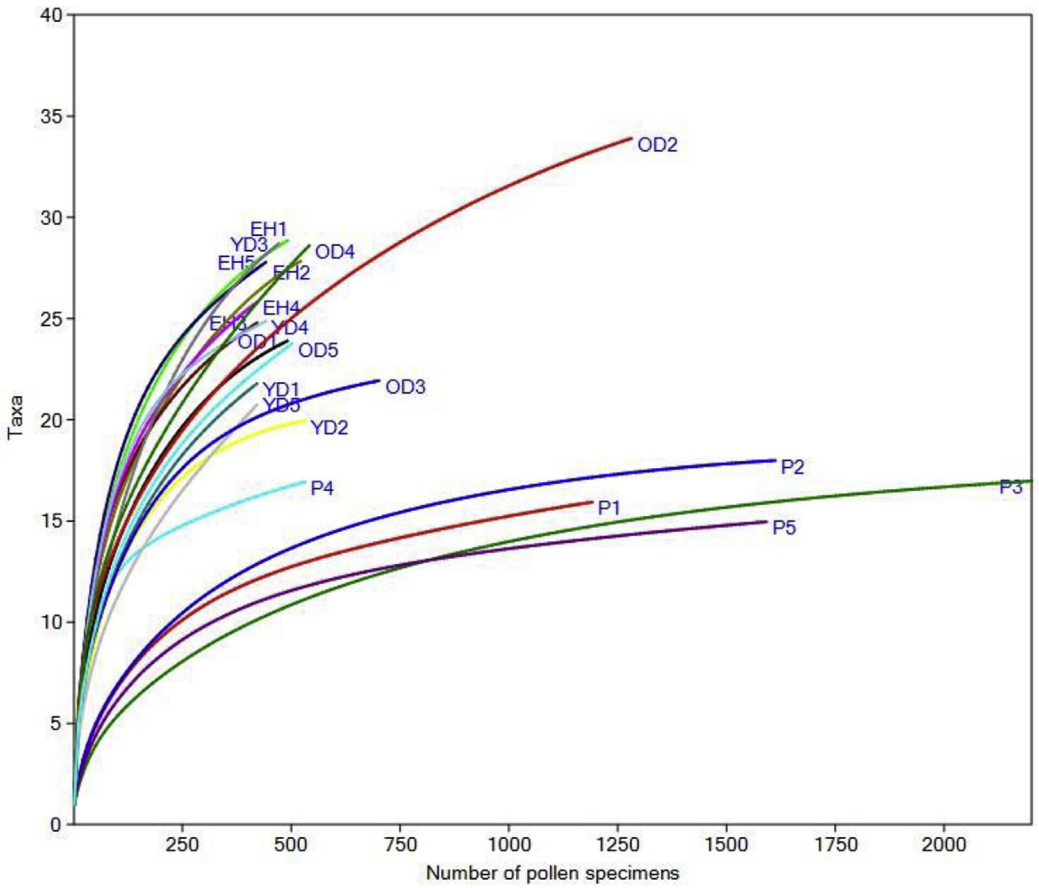


**Fig. 6.** Comparison of rarefied richness of selected samples from different periods. P: present surface soil samples from Haligu, EH: early Holocene samples from this study (9.4–9.2 cal. ka BP), YD: YD samples from this study (12.5 cal. ka BP), OD: Older Dryas samples from Wenhai core (17.1–16.3 cal. ka BP).

PZ 5, with frequent fluctuations in relative humidity from PZ1 to PZ5.

## 4. Discussion and conclusions

### 4.1. Vegetation responses to the YD climatic oscillation at Haligu

As a global climate event, the abrupt characteristics of the YD are well documented in multiple geological archives. For example, the LOI value of the Splan Lake core in Canada, North America, suddenly dropped from 19% to 4% in just 25 years, suggesting the beginning of the YD event, and the relative abundance of *Picea* pollen sharply changed from >55% to <15% within 50 years, indicating a climate warming after the termination of this event (Mayle and Cwynar, 1995). A $\delta^{18}O$ record from mollusk shells at Twiss Marl Pond in Central North America shows a negative shift of 1.3‰, representing a 3 °C decrease in mean annual air temperature at the onset of the YD, and a positive shift of 2‰, indicating a 6 °C increase in mean annual air temperature at the end of the YD, followed by the Holocene (Yu and Eicher, 1998). The Greenland ice core, GISP2, recorded that snow accumulation doubled in 1–3 years at the end of the YD (Alley et al., 1993). The Atlantic Cariaco basin recorded a thin varved sediment in less than a decade implying the termination of the YD (Hughen et al., 1996). Stalagmite $\delta^{18}O$ results from Hulu Cave in Nanjing, China indicated that the durations of the initiation and termination of the YD lasted less than 20 years and 10 years, respectively (Wang et al., 2001).

The palynological study and LOI analysis in this paper also detect a signal of the abrupt initiation and termination of the YD event. The relative abundance of *Picea* and *Abies* pollen is 30.4% at the depth of 730–728 cm (12.9 cal. ka BP), then rapidly increases up to 39.2% at 728–726 cm, accompanied by a sharp drop in LOI value from 44.2% to 18.2% within about 30 years, which may be a cooling signal and indicates the beginning of the YD. Pollen evidence also captures the signal of termination of this event. For example, the relative abundance of *Picea* and *Abies* pollen suddenly decreases from 37.1% at 606–604 cm (11.2 cal. ka BP) to 25.3% at 604–602 cm and 19.7% at 602–600 cm (Fig. 5b), which suggests climate warming and signifies the end of the YD. The temperature variation curve also points to a notable climate warming at 11.2 cal. ka BP (Fig. 5a). Based on the sedimentation rates of the studied Haligu core, the samples between 730 and 600 cm represent a resolution of about 27 years, so we calculate the duration of both the initiation and termination of the YD at approximately 30 years each. Therefore we estimate that the YD event occurred between 12.9 and 11.2 cal. ka BP in this core.

In the present study, palynological zones PZ 1 (12.9–12.4 cal. ka BP), PZ 2 (12.4–11.9 cal. ka BP) and PZ 3 (11.9–11.2 cal. ka BP) lie within the YD event. The axes PCA1 and PCA2 scores reflect changes in temperature and relative humidity during the YD and early Holocene, and indicate that the area experienced cold-dry, cold-wet, and cold-dry conditions during the three periods of the YD. Under cold conditions, plant diversity is positively related to relative humidity (Fig. S6), and both humidity and diversity show consistent trends (Fig. 5d–h). The ecological indices illustrate that the plant diversity in PZ 1 and PZ 2 is lower than in PZ 3 (Fig. 5e–h),

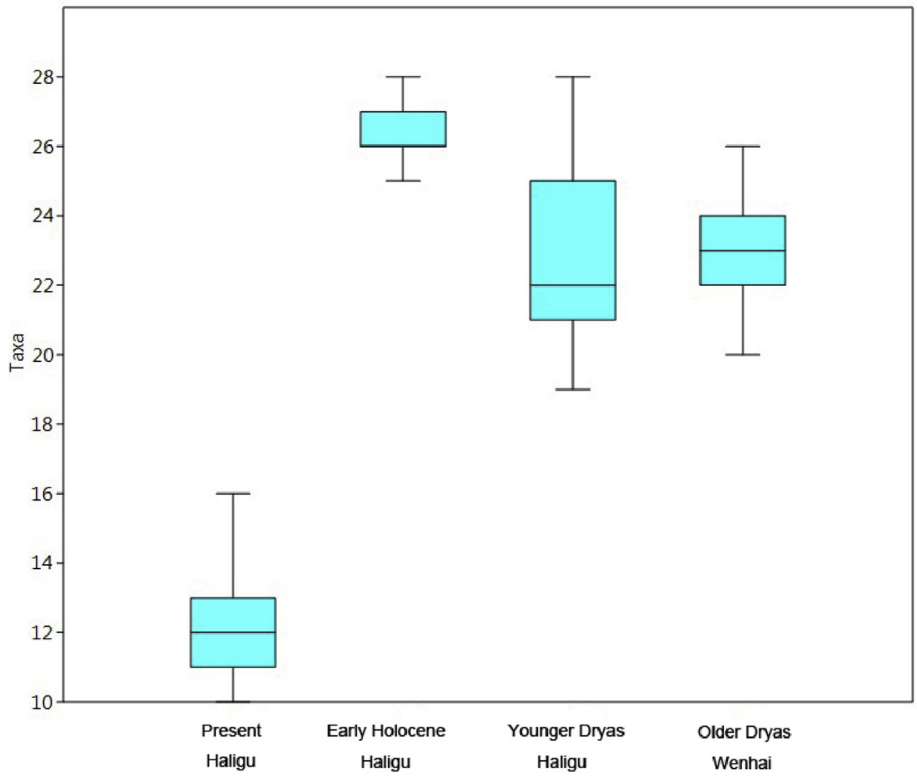


**Fig. 7.** Rarefied richness expressed as boxplots based on selected fossil and extant pollen data (Boxes indicate first (25%) and third (75%) quartiles; bars indicate the median quartile).

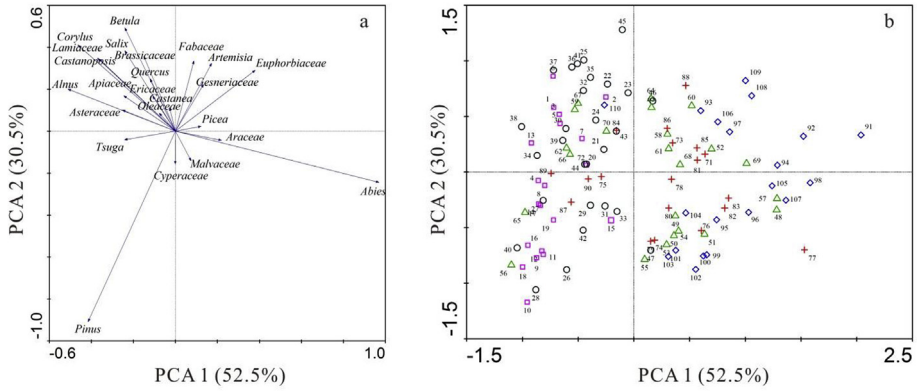


**Fig. 8.** PCA ordination of pollen relative abundance. a. PCA biplot of pollen taxa. b. PCA biplot of pollen samples.

while rarefaction analysis suggests that the species richness in most YD samples is lower than the early Holocene samples (Figs. 6 and 7). In order to investigate the vegetation changes across these three periods, we review the ecological preferences of the dominant taxa recovered from Haligu core. For example, today, *Pinus* mainly grows below 3200 m a. s. l. elevation in SW China and prefers fairly warm and moderately dry conditions (Wang et al., 2007). *Tsuga* is today a cold-tolerant and hygrophilous taxon corresponding to mean annual temperatures of 8.4–10.5 °C and mean annual precipitation of about 1000 mm in Yunnan (WGYV, 1987), with a distribution range from 2200 m to 3500 m. *Abies* and *Picea* are today microthermic genera with mean annual temperature requirements of 2–8 °C and 2.1–9.4 °C, respectively, in the mountains of SW China (CCCV, 1980; Jarvis, 1993; Fang et al., 2011). In Yunnan these genera grow between elevations of 2200–4200 m and 2300–3800 m respectively. Cyperaceae are today abundant in wetlands and surrounding areas, including the open, high altitude meadows of the Jade Dragon Snow Mountain. The high relative abundance of Cyperaceae pollen may indicate humid conditions (Sun et al., 2003). Based on the relative abundance and pollen concentration changes of dominant taxa (Figs. 3 and 4) and their ecological preferences, it is notable that the vegetation is characterized by needle-leaved forest during all three periods, but the community composition and dominant components differ between them. For example, the vegetation community is mainly composed of *Pinus*, *Abies*, *Picea,* and Cyperaceae in PZ 1, changes to *Pinus*, *Abies*, *Tsuga,* and Cyperaceae in PZ 2, and to *Pinus* and *Abies* in PZ 3. After the YD, as the climate becomes warmer, marking the onset of Holocene (PZ 4 and 5), the vegetation is mostly dominated by *Pinus*, together with sharp decreases in abundance of *Abies* and *Picea,* and

gradual increases in that of some temperate taxa such as *Betula, Quercus* and *Salix* (Fig. 9).

### 4.2. Comparison of vegetation responses to the YD at regional and global levels

During the past decade, several studies have recorded the occurrence of the YD event in lake sediments from different altitudes in the Hengduan Mountains (Shen et al., 2006; Xiao et al., 2014a, 2014b, 2015), enabling us to make comparisons with previous investigations to reveal vegetation responses to the YD event and possible ecological mechanisms along altitudinal gradients (Fig. 9). At Qinghai Lake (1885 m), the vegetation is characterized by a dominance of evergreen *Quercus* broad-leaved forest before and during the YD, followed by increases in abundance of *Betula* and *Alnus* and decreases in that of *Pinus*, evergreen and deciduous *Quercus* after the YD (Xiao et al., 2015). At Erhai Lake (1974 m), the vegetation shifts from deciduous broad-leaved forest (mainly comprising *Betula* and *Quercus*) during the YD to mixed needle-leaved and broad-leaved forest after the YD (Shen et al., 2006). In the present study, the vegetation around Haligu (3218 m) changes from *Pinus-Abies-Picea* forest during the YD to *Pinus*-dominated forest after the YD. *Picea, Abies* and *Betula* forest occupies the surroundings of Tiancai Lake (3898 m) before the YD, accompanied by a retreat of alpine meadow. This vegetation is characterized by the marked expansion of alpine meadow during the YD, which was replaced by *Picea* and *Abies* forest and alpine *Rhododendron* shrubland after the YD (Xiao et al., 2014a, 2014b).

Regional comparison indicates that the Hengduan Mountains subalpine conifer forest (composed of two primary arboreal taxa,

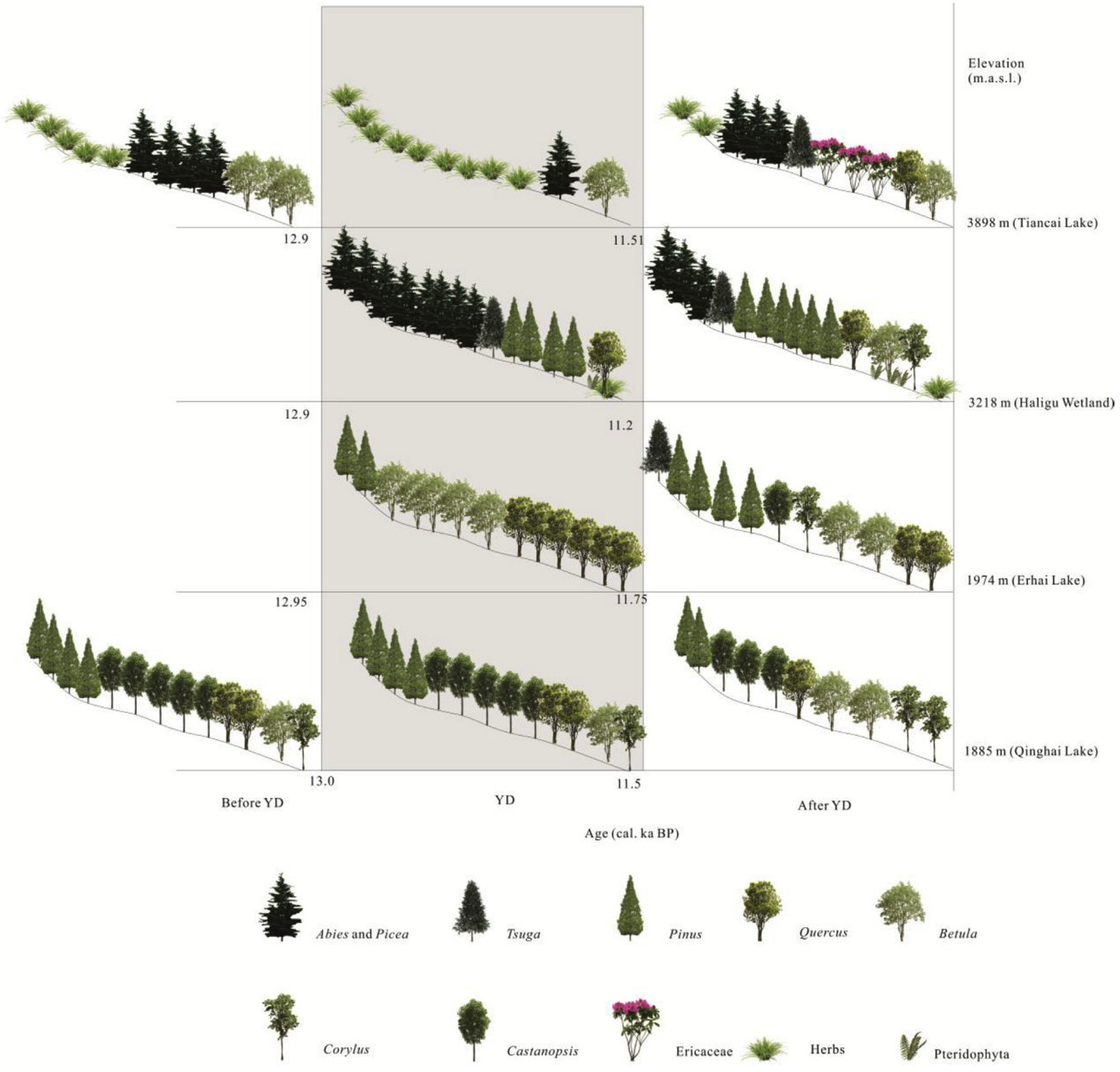


**Fig. 9.** Schematic diagram showing various responses of vegetation to the YD event along altitudinal gradients in the Hengduan Mountains.

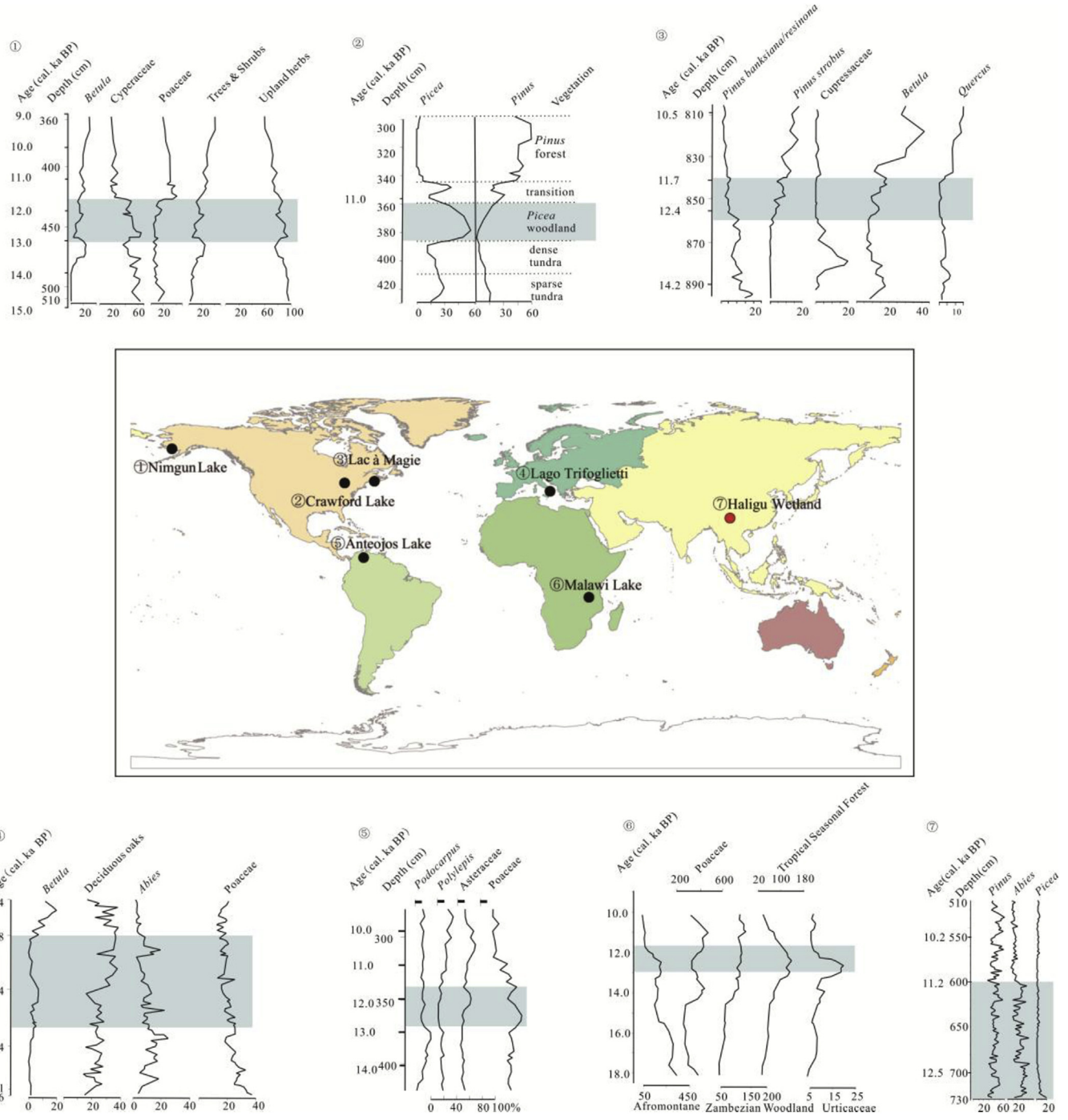


**Fig. 10.** A global comparison of vegetation responses to the YD event. Curves showing the major changes in palynological assemblages are redrawn from Lac à Magie, Canada (Mayle et al., 1995), Crawford Lake, Central North America (Yu and Eicher, 1998), Nimgun Lake, Southwestern Alaska (Hu et al., 2002), Lake Anteojos, South America (Rull et al., 2010), Lake Malawi, East Africa (Ivory et al., 2012), Lago Trifoglietti, Southern Italy (Beaulieu et al., 2017), and the present study (Haligu Wetland, Hengduan Mountains). The YD event is marked by grey rectangles.

*Picea* and *Abies*) migrated downhill during the YD cold period and uphill in the warming early Holocene. A parallel response of alpine timberline vegetation (mainly *Abies*, *Picea* and *Pinus*) has been documented as a response to the YD climate oscillation in the Colorado Rocky Mountains, USA (Reasoner and Jodry, 2010). Differences in vegetation feedback at different altitudes may be caused by two crucial climatic factors temperature and moisture. In the Hengduan Mountains, temperature decreases with ascending altitude but humidity and precipitation increase. As indicated in Fig. 9, the vegetation is mainly dominated by needle-leaved forest, consisting of cold-tolerant taxa *Abies* and *Picea* and the more hygrophilous taxon *Tsuga* at high altitudes (above 2500 m). Temperate taxa *Quercus*, *Castanopsis* and *Betula* are the main components in evergreen/deciduous broad-leaved forest at relatively low altitudes (below 2000 m). During the YD interval, changes in patterns of atmospheric and oceanic circulation triggered a rapid cooling in the Northern Hemisphere (Bakke et al., 2009). Moreover, precipitation reduced in the Hengduan

Mountains due to the weak Southwest monsoon in this period (Xiao et al., 2014a, 2014b; Sinha et al., 2005; Rawat et al., 2015). Therefore, our results suggest that the needle-leaved taxa *Abies* and *Picea,* and the temperate broad-leaved taxa *Quercus*, *Castanopsis,* and *Betula* are sensitive to decreases in temperature, while *Tsuga* is highly susceptible to changes in moisture.

Interestingly, we found that the response of vegetation to the YD event throughout the world mainly appears to comprise changes in community composition and the relative abundance of dominant taxa (Fig. 10). For example, a pollen record from Lago Trifoglietti, Southern Italy suggests that the YD did not greatly impact vegetation dynamics, evidenced by a resilient expansion of oak forest at lower altitude (1048 m a. s. l.) along with a moderate increase in abundance of steppe taxa, followed by a phase of *Betula* expansion in the early Holocene (Beaulieu et al., 2017). Palynological assemblages from two lakes in Ontario, Central North America, indicate that the vegetation was dominated by *Picea* woodland during the YD, shifting to *Pinus* forest after the YD (Yu and Eicher, 1998). The shrub-tundra occurring around Lac à Magie, Canada from the last-glacial period to early Holocene, showed notable floristic changes (Mayle and Cwynar, 1995). Similarly, páramo herbs and shrubs, Andean forest and *Polylepis* forests surrounded Lake Anteojos, Venezuela, in northernmost South America, during the Bølling/Allerød-early Holocene, where abrupt shifts in the relative abundance of dominant taxa *Podocarpus*, *Polylepis* and Poaceae were clearly documented as a response to the YD event (Rull et al., 2015). At Lake Malawi, southeast Africa, the expansion of tropical seasonal forest and afromontane forest and reduction of grassland are regarded as a response to the YD cooling, and the climate warming at the termination of the YD caused the rapid expansion of grassland accompanied by a decline in tropical seasonal forest and afromontane forest (Ivory et al., 2012). In the present study, the vegetation at Haligu was dominated by needle-leaved forest during the late glacial/early Holocene, with a maximum abundance of, and abrupt decline in, *Abies* and *Picea* as a response to the onset and end of the YD. To summarize, the YD event is a global phenomenon which has impacted on vegetation community composition and dominant taxa, characterized by an abrupt change in the relative abundance of temperature-sensitive arboreal taxa (e.g., *Abies, Picea, Podocarpus*) and herbaceous plants (e.g., Poaceae) at most sites (Fig. 10). However, the YD event is not sufficient to cause a significant change in vegetation type, which is probably because of the short duration of the YD. Climate forcing (e.g., temperature and moisture) and geomorphology (e.g., altitude, slope and aspect) may play an important role in the regional variation of vegetation response to this event.

### 4.3. Lessons for future biodiversity conservation

The observations of rapid climatic change in this paper could be useful as past analogs for the future biotic responses and biodiversity conservation in the Hengduan Mountains, as well as in similar mountain ecosystems worldwide. It is likely that temperature-sensitive plant taxa such as *Abies*, *Picea,* and *Quercus* may migrate up or downhill as a response to climate warming or cooling. Therefore, significant changes in the altitudinal ranges of these plants can be expected in the near future and these will interact with both biodiversity (e.g., pollinating insects) and human activities (e.g., harvesting of fuelwood and timber) in the studied region. For example, the local people (Naxi and Yi ethnic minorities) of the Jade Dragon Snow Mountain today use large oak trees in construction and make heavy use of coppiced oak branches for fuelwood (Song et al., 2012).

The results obtained in the present paper show that relative humidity was an important factor influencing plant diversity in the past. The glaciers of the Hengduan Mountains played an important role in hydrological processes of this region. During recent decades, glaciers have been melting and retreating rapidly due to increased temperatures in southwestern China. For example, the average annual runoff in the Hailuo Creek Basin was 2114 mm from 1952 to 2009, of which glacial melting accounted for about 1078 mm (Zhu et al., 2016). The Hailuogou glacier retreated at a speed of 23.6 m/a between 1930 and 2006, and the glacier area on Jade Dragon Snow Mountain was reduced by 0.07 $km^2$/a between 1957 and 1999 (Li et al., 2011). Retreating glaciers will almost certainly have effects on water availability which will impact plant diversity and regional vegetation composition.

Recent studies have documented changes in the flowering phenology of *Rhododendron* species (Ericaceae) and rosaceous plants (Rosaceae) indicating that climate change has already impacted the biota of the Hengduan Mountains over the past century (Hart et al., 2014; Yu et al., 2016). For example, Hart et al. (2014) used 10,295 herbarium specimens of Himalayan *Rhododendron* to investigate climate-driven changes in flowering time, and found that annual warming may advance flowering through positive effects on overwintering bud formation, whereas fall warming may delay flowering through an impact on chilling requirements. Yu et al. (2016) examined specimens of *Rosa* and *Cotoneaster* species collected between the 1920s and 2010s in the Hengduan Mountains to analyze changes of flowering phenology and flower size and to evaluate the effects of global change on plants in this region. Their observations revealed that the flowering phenology of *Rosa* and *Cotoneaster* varied with altitude and showed different changes as a response to increased temperature in the past century, i.e., the flowering phenology of *Cotoneaster* was delayed in recent years, but flowering phenology of *Rosa* showed no significant change. Given the uncertainty that rapid climate change creates, we should make greater efforts to conserve plant diversity. Both seed banks such as the Germplasm Bank of Wild Species in Southwest China at the Kunming Institute of Botany, Chinese Academy of Sciences, and cultivation in Botanic Gardens provide safe havens for threatened species and potential sources of material for habitat restoration, which may need to take account of altitudinal changes in vegetation zones.

## Acknowledgments

We gratefully acknowledge financial support from the National Key R & D Program of China (No. 2017YFC0803803), China National Key Basic Research Program (No. 2014CB954201), National Natural Science Foundation of China (No. 41271222), and a Visiting Scholarship funded by the China Scholarship Council (No. 201204910043). The Royal Botanic Garden Edinburgh (RBGE) is supported by the Scottish Government's Rural and Environmental Science and Analytical Services Division.

## Appendix A. Supplementary data

Supplementary data related to this article can be found at https://doi.org/10.1016/j.quascirev.2018.06.007.

## References

Alley, R.B., Meese, D.A., Shuman, C.A., Gow, A.J., Taylor, K.C., Grootes, P.M., White, J.W.C., Ram, M., Waddington, E.D., Mayewski, P.A., Zielinski, G.A., 1993. Abrupt increase in snow accumulation at the end of the Younger Dryas event. Nature 362, 527–529.

Baillie, M.G.L., Reimer, P.J., 2004. IntCal04 terrestrial radiocarbon age calibration, 0–26 cal kyr BP. Radiocarbon 46, 1029–1058.

Bakke, J., Lie, Ø., Heegaard, E., Dokken, T., Haug, G.H., Birks, H.H., Dulski, P., Nilsen, T.,

2009. Rapid oceanic and atmospheric changes during the Younger Dryas cold period. Nat. Geosci. 2, 202–205.
Ballenger, J.A.M., Holliday, V.T., Kowler, A.L., Reitze, W.T., Prasciunas, M.M., Miller, D.S., Windingstad, J.D., 2011. Evidence for Younger Dryas global climate oscillation and human response in the American Southwest. Quat. Int. 242, 502–519.
Barnosky, A.D., Koch, P.L., Feranec, R.S., Wing, S.L., Shabel, A.B., 2004. Assessing the causes of late Pleistocene extinctions on the continents. Science 306, 70–75.
Beaulieu, J.L., Brugiapaglia, E., Joannin, S., Guiter, F., Zanchetta, G., Wulf, S., Peyron, O., Bernardo, L., Didier, J., Stock, A., Rius, D., Magny, M., 2017. Late glacial-Holocene abrupt vegetation changes at Lago Trifoglietti in Calabria, Southern Italy: the setting of ecosystems in a refugial zone. Quat. Sci. Rev. 158, 44–57.
Berglund, B.E., Ralska-Jasiewiczowa, M., 1986. Pollen analysis and pollen diagrams. In: Berglund, B.E. (Ed.), Handbook of Holocene Palaeoecology and Palaeohydrology. John Wiley & Sons, Chichester, pp. 455–496.
Birks, H.J.B., Gordon, A.D., 1985. Numerical Methods in Quaternary Pollen Analysis. Academic Press, London.
Blaauw, M., Christen, A., 2011. Flexible paleoclimate age-depth models using an autoregressive gamma process. Bayesian Anal 6 (3), 457–474.
Bond, G., Broecker, W., Johnsen, S., McManus, J., Labeyrie, L., Jouzel, J., Bonanl, G., 1993. Correlations between climate records from North Atlantic sediments and Greenland ice. Nature 365, 143–147.
Boufford, D.E., van Dijk, P.P., 2004. Mountains of Southwest China. In: Mittermeter, R.A., Gil, P.R., Hoffman, M., et al. (Eds.), Hotspot Revisited: Earth's Biologically Richest and Most Endangered Ecoregions, 2nd. Cemex, Mexico, pp. 159–164.
Bronk, R., 2005. OxCal Program v3.10. University of Oxford Radiocarbon Accelerator Unit.
Buczkó, K., Magyari, E., Hübener, T., Braun, M., Bálint, M., Tóth, M., Lotter, A.F., 2012. Responses of diatoms to the Younger Dryas climatic reversal in a South Carpathian mountain lake (Romania). J. Paleolimnol. 48, 417–431.
CCCV (Compilation Committee of Chinese Vegetation), 1980. Vegetation of China. Science Press, Beijing (in Chinese).
Clark, P.U., Pisias, N.G., Stocker, T.F., Weaver, A.J., 2002. The role of the thermohaline circulation in abrupt climate change. Nature 415, 863–869.
Dansgaard, W., Johnsen, S.J., Clausen, H.B., Dahl-Jensen, D., Gundestrup, N.S., Hammer, C.U., Hvidberg, C.S., Steffensen, J.P., Sveinbjörnsdottir, A.E., Jouzel, J., Bond, G., 1993. Evidence for general instability of past climate from a 250-kyr ice-core record. Nature 364, 218–220.
Dean Jr., W.E., 1974. Determination of carbonate and organic matter in calcareous sediments and sedimentary rocks by loss on ignition: comparison with other methods. J. Sediment. Petrol. 44, 242–248.
Fang, J.Y., Wang, Z.H., Tang, Z.Y., 2011. Atlas of Woody Plants in China: Distribution and Climate. Springer & Higher Education Press, Berlin & Beijing.
Feng, J.M., Wang, X.P., Xu, C.D., Yang, Y.H., Fang, J.Y., 2006. Altitudinal patterns of plant diversity and community structure on Yulong Mountains, Yunnan, China. J. Mt. Sci. 24, 110–116.
Foster, G.C., Chiverrell, R.C., Harvey, A.M., Dearing, J.A., Dunsford, H., 2008. Catchment hydro-geomorphological responses to environmental change in the Southern Uplands of Scotland. Holocene 18, 935–950.
Frey, D., Deevey, E.S., 1998. Numerical tools in palaeolimnology-progress, potentialities and problems. J. Paleolimnol. 20, 307–332.
Grimm, E., 2011. In: Tilia Software 1.7.14. Research and Collection Center Springfield, Illinois.
Hart, R., Salick, J., Ranjitkar, S., Xu, J.X., 2014. Herbarium specimens show contrasting phenological responses to Himalayan climate. P. Natl. Acad. Sci. USA 111, 10615–10619.
Hu, F.S., Lee, B.Y., Kaufman, D.S., Yoneji, S., Nelson, D.M., Henne, P.D., 2002. Response of tundra ecosystem in southwestern Alaska to Younger-Dryas climatic oscillation. Global Change Biol. 8, 1156–1163.
Hughen, K.A., Overpeck, J.T., Peterson, L.C., Trumbore, S., 1996. Rapid climate changes in the tropical Atlantic region during the last deglaciation. Nature 380, 51–54.
IBCAS (Institute of Botany, Chinese Academy of Sciences), 1976. Spore Pteridophytorum Sinicorum. Science Press, Beijing (in Chinese).
IBSC-IBCAS (Institute of Botany and South China Institute of Botany, Chinese Academy of Sciences), 1982. Angiosperm Pollen Flora of Tropic and Subtropic China. Science Press, Beijing (in Chinese).
Ivory, S.J., Lézine, A.M., Vincens, A., Cohen, A.S., 2012. Effect of aridity and rainfall seasonality on vegetation in the southern tropics of East Africa during the Pleistocene/Holocene transition. Quat. Res. 77, 77–86.
Jarvis, D.I., 1993. Pollen evidence of changing Holocene monsoon climate in Sichuan Province, China. Quat. Res. 39, 325–337.
Johnsen, S.J., Clausen, H.B., Dansgaard, W., Fuhrer, K., Gundestrup, N., Hammer, C.U., Iversen, P., Jouzel, J., Stauffer, B., Steffensen, J.P., 1992. Irregular glacial interstadials recorded in a new Greenland ice core. Nature 359, 311–313.
Jomelli, V., Favier, V., Vuille, M., Braucher, R., Martin, L., Blard, P.-H., Colose, C., Brunstein, D., He, F., Khodri, M., Bourlès, D.L., Leanni, L., Rinterknecht, V., Grancher, D., Francou, B., Ceballos, J.L., Fonseca, H., Liu, Z., Otto-Bliesner, B.L., 2014. A major advance of tropical Andean glaciers during the Antarctic cold reversal. Nature 513, 224–228.
Kramer, A., Herzschuh, U., Mischke, S., Zhang, C., 2010. Holocene treeline shifts and monsoon variability in the Hengduan Mountains (southeastern Tibetan Plateau), implications from palynological investigations. Palaeogeogr. Palaeoclimatol. Palaeoecol. 286, 23–41.
Li, Z.X., He, Y.Q., An, W.L., Song, L.L., Zhang, W., Catto, N., Wang, Y., Wang, S.J., Liu, H.C., Cao, W.H., Theakstone, W.H., Wang, S.X., Du, J.K., 2011. Climate and glacier change in southwestern China during the past several decades. Environ. Res. Lett. 6 https://doi.org/10.1088/1748-9326/6/4/045404.
Mayle, F.E., Cwynar, L.C., 1995. Impact of the Younger Dryas cooling event upon lowland vegetation of Maritime Canada. Ecol. Monogr. 65, 129–154.
Miller, A.I., Foote, M., 1996. Calibrating the Ordovician radiation of marine life: implications for Phanerozoic diversity trends. Paleobiology 22, 304–309.
Mook, W.G., 1986. Recommendations/resolutions adopted by the twelfth international radiocarbon conference. Radiocarbon 28, 799.
Moore, P.D., Webb, J.A., Collinson, M.E., 1991. Pollen Analysis, second ed. Blackwell Scientific Publications, Oxford, pp. 42–46.
Oksanen, J., Blanchet, F.G., Kindt, R., Legendre, P., Minchin, P.R., O'Hara, R.B., Simpson, G.L., Solymos, P., Stevens, M.H.H., Wagner, H., 2016. Vegan: Community Ecology Package. R Package Version 2.3–5.
Partin, J.W., Quinn, T.M., Shen, C.C., Okumura, Y., Cardenas, M.B., Siringan, F.P., Banner, J.L., Lin, K., Hu, H.M., Taylor, F.W., 2015. Gradual onset and recovery of the Younger Dryas abrupt climate event in the tropics. Nat. Commun. 6 https://doi.org/10.1038/ncomms9061.
Rawat, S., Gupta, A.K., Sangode, S.J., Srivastava, P., Nainwal, H.C., 2015. Late pleistocene-holocene vegetation and indian summer monsoon record from the lahaul, northwest himalaya, India. Quat. Sci. Rev. 114, 167–181.
R Core Team, 2014. R: a Language and Environment for Statistical Computing. R Foundation for Statistical Computing, Vienna, Austria. Http://www.r-project.org.
Reasoner, M.A., Jodry, M.A., 2010. Rapid response of alpine timberline vegetation to the Younger Dryas climate oscillation in the Colorado Rocky Mountains, USA. Geology 28, 51–54.
Rull, V., Stansell, N.D., Montoya, E., Bezada, M., Abbott, M.B., 2010. Palynological signal of the younger Dryas in the tropical venezuelan andes. Quat. Sci. Rev. 29, 3045–3056.
Rull, V., Vegas-Vilarrúbia, T., Montoya, E., 2015. Neotropical vegetation responses to Younger Dryas climates as analogs for future climate change scenarios and lessons for conservation. Quat. Sci. Rev. 115, 28–38.
Sanders, H.L., 1968. Marine benthic diversity: a comparative study. Am. Nat. 102, 243–282.
Shakun, J.D., Carlson, A.E., 2010. A global perspective on last glacial maximum to Holocene climate change. Quat. Sci. Rev. 29, 1801–1816.
Shen, J., Jones, R.T., Yang, X.D., Dearing, J.A., Wang, S.M., 2006. The Holocene vegetation history of Lake Erhai, Yunnan province southwestern China: the role of climate and human forcings. Holocene 16, 265–276.
Sinha, A., Cannariato, K.G., Stott, L.D., Li, H.C., You, C.F., Cheng, H., Edwards, R.L., Singh, I.B., 2005. Variability of Southwest Indian summer monsoon precipitation during the Bølling-Ållerød. Geology 33, 813–816.
Song, X.Y., Yao, Y.F., Wortley, A.H., Paudayal, K.N., Yang, S.H., Li, C.S., Blackmore, S., 2012. Holocene vegetation and climate history at Haligu on the jade dragon snow mountain, yunnan, SW China. Climatic Change 113, 841–866.
Sun, H., 2002. Evolution of arctic-tertiary flora in himalayan-hengduan mountains. Acta Bot. Yunnanica 24, 671–688.
Sun, X.J., Luo, Y.L., Huang, F., Tian, J., Wang, P.X., 2003. Deep-sea pollen from the south China sea: pleistocene indicators of East asian monsoon. Mar. Geol. 201, 97–118.
ter Braak, C.J.F., Smilauer, P., 2002. CANOCO Reference Manual and Cano-draw for Windows User's Guide: Software for Canonical Community Ordination (Version 4.5). Microcomputer Power, Ithaca.
Wang, F.X., Chen, N.F., Zhang, Y.L., Yang, H.Q., 1995. Pollen Flora of China. Science Press, Beijing (in Chinese).
Wang, H., Zhang, C.Q., Li, D.Z., Xue, R.G., Yang, Q.E., 2007. Checklist of Seed Plants of Lijiang Alpine Botanic Garden. Yunnan Science and Technology Press, Kunming (in Chinese).
Wang, Y.J., Cheng, H., Edwards, R.L., An, Z.S., Wu, J.Y., Shen, C.C., Dorale, J.A., 2001. A high-resolution absolute-dated late Pleistocene Monsoon record from Hulu Cave, China. Science 294, 2345–2348.
WGYV (Writing Group of Yunnan Vegetation), 1987. Vegetation of Yunnan. Science Press, Beijing (in Chinese).
Wu, Z.Y., 1988. Hengduan Mountain flora and her significance. J. Jpn. Bot. 63, 297–311.
Xiao, X.Y., Haberle, S.G., Shen, J., Yang, X.D., Han, Y., Zhang, E.L., Wang, S.M., 2014a. Latest Pleistocene and Holocene vegetation and climate history inferred from an alpine lacustrine record, northwestern Yunnan Province, southwestern China. Quat. Sci. Rev. 86, 35–48.
Xiao, X.Y., Haberle, S.G., Yang, X.D., Shen, J., Han, Y., Wang, S.M., 2014b. New evidence on deglacial climatic variability from an alpine lacustrine record in northwestern Yunnan Province, southwestern China. Palaeogeogr. Palaeoclimatol. Palaeoecol. 406, 9–21.
Xiao, X.Y., Shen, J., Haberle, S.G., Han, Y., Xue, B., Zhang, E.L., Wang, S.M., Tong, G.B., 2015. Vegetation, fire, and climate history during the last 18500 cal a BP in south-western Yunnan Province, China. J. Quat. Sci. 30, 859–869.
Yao, Y.F., Song, X.Y., Wortley, A.H., Blackmore, S., Li, C.S., 2015. A 22570-year record of vegetational and climatic change from Wenhai Lake in the Hengduan Mountains biodiversity hotspot, Yunnan, Southwest China. Biogeosciences 12, 1525–1535.
Yao, Y.F., Song, X.Y., Wortley, A.H., Wang, Y.F., Blackmore, S., Li, C.S., 2017. Pollen-based reconstruction of vegetational and climatic change over the past ~30 ka

at Shudu Lake in the Hengduan Mountains of Yunnan, southwestern China. PLoS One 12. https://doi.org/10.1371/journal.pone.0171967 e0171967.
Yu, Q., Jia, D.R., Tian, B., Yang, Y.P., Duan, Y.W., 2016. Changes of flowering phenology and flower size in rosaceous plants from a biodiversity hotspot in the past century. Sci. Rep. 6 https://doi.org/10.1038/srep28302.
Yu, Z.C., Eicher, U., 1998. Abrupt climate oscillations during the last deglaciation in central North America. Science 282, 2235–2238.
Zhang, E.L., Sun, W.W., Zhao, C., Wang, Y.B., Xue, B., Shen, J., 2015. Linkages between climate, fire and vegetation in southwest China during the last 18.5 ka based on a sedimentary record of black carbon and its isotopic composition. Palaeogeogr. Palaeoclimatol. Palaeoecol. 435, 86–94.
Zhu, G.F., He, Y.Q., Qin, D.H., Gao, H.K., Pu, T., Chen, D.D., Wang, K., 2016. The impacts of climate change on hydrology in a typical glacier region-A case study in Hailuo Creek watershed of Mt. Gongga in China. Sci. Cold Arid Reg 8, 227–240.